



Quantum Lattice Simulations PHYSICS: Microcircuit Particle Formation and Observable Macroscopic Irreversible Time - A Discrete Lagrangian with Cellular Automata Framework

Iyer R*

Environmental Materials Theoretical Physicist, Department of Physical Mathematics Sciences Engineering Project Technologies, Engineeringinc International Operational Teknet Earth Global, Tempe, Arizona, United States of America

Research Article

Volume 10 Issue 1

Received Date: January 22, 2026

Published Date: February 10, 2026

DOI: [10.23880/psbj-16000287](https://doi.org/10.23880/psbj-16000287)

***Corresponding author:** Rajan Iyer, Environmental Materials Theoretical Physicist, Department of Physical Mathematics Sciences Engineering Project Technologies, Engineeringinc International Operational Teknet Earth Global, Tempe, Arizona, United States of America; ORCID ID#:0000-0002-5729-1393, Email: engginc@msn.com

Abstract

We develop a unified simulation framework for particle formation in quantum lattice systems using discrete Lagrangian mechanics and quantum cellular automata (QCA), to explore the particle formation and multi-scale time asymmetry, building on the author's recent paper on early universe magneto-gravitational genesis mechanism. The model introduces a dual-regime time epochs scales: microscopically reversible "microcircuits" dominate below a characteristic time scale $\tau = 10^{-24} \text{ s}$, corresponding to a regime of spatial cutoff $\ell_c = 3 \times 10^{-16} \text{ m}$, while macroscopic "macrocircuits" above this scale exhibit effective irreversibility. We simulate a typical nonlinear scalar field in 1D and 2D lattices using variational integrators, Lorentz-violating spatial derivatives, and an energy-density threshold rule encoding emergent particle events. Here, entropy-based information proxy approximates local field complexity, while it effectively correlates with irreversible behavior. Results output with numerical simulations reveal the distinct temporal-spatial dynamics: appearing fields having evolution soliton-like reversible interactions at sub - scales ($< 3 \times 10^{-16} \text{ m}$), while above ℓ_c : irreversible dynamics, clustering, as well as persistent particle formations emerge at macro scales. These findings support the feasibility of a dual-scale lattice field theory from first principles and provide a foundation for topologically structured quantum field architectures relevant to spacetime modeling and condensed-matter analogues, especially quantum cellular automata.

Keywords: Quantum Lattice; Microcircuits; Macrocircuits; Cellular Automata; Discrete Lagrangian Mechanics; Particle Formation; Entropy Proxy; Superluminal Condensate; Time Irreversibility; Quantum Field Simulations; Early Universe

Abbreviations

SMGC: Superluminal Magnetic General Condensate; QCA: Quantum Cellular Automata; CPTP: Completely Positive

Trace-Preserving; QCLI: Quantum Circuit Lyapunov Indicator; FFT: Fast Fourier Transforms; RG: Renormalization-Group; AI: Artificial Intelligence.

Introduction

Extensive physical literature survey research preceded this pioneering article to understand the processes of mechanisms naturally operating in early universe [1-96]. The author has peer published breakthrough early universe quantum cosmological mathematical physics general simulation model, advancing “baryon asymmetric process” symmetry breaking Superluminal Magnetic General Condensate (SMGC) via the Hod-PDP Particle Genesis Mechanism into a quantitatively unified description of the early universe, where superluminal coherence, Lorentz-violating dynamics, and semiclassical tunneling jointly govern the emergence of matter alongside structure [35]. The reconciliation typically of microscopically time-symmetric laws well with macroscopically irreversible behavior remains a fundamental challenge in theoretical physics now. Standard formulations - Newtonian mechanics, Hamiltonian flows, as well as unitary quantum evolution - are fully reversible, yet observable macroscopic processes display a well-defined arrow of time [94]. This tension becomes especially acute in attempts to model particle formation from vacuum fluctuations, nonlinear field excitations, or exotic condensate phenomena potentially associated with superluminal or Lorentz-violating sectors [72].

Recent work in quantum cellular automata (QCA) has shown that unitary quantum dynamics can then be encoded on discrete spacetime substrates without recourse to the normal continuum limits [3,13]. Parallel developments in discrete Lagrangian mechanics as well as variational integrators demonstrate that discretized actions can preserve symmetries and yield stable, physically consistent general fields equations [54]. Together, these approaches establish a natural platform for exploring emergent structures - such as localized excitations, solitons, or particle-like objects - within non-perturbative lattice dynamics. These two frameworks complement each other, whereby the smooth nonlinear dynamics can capture variational field evolution, while QCA rules encode localized discrete events and history tracking.

We propose a hybrid model combining discrete framework field-theoretic variational evolutions with QCA-style threshold rules. Our guiding hypothesis shows that dynamics exhibit dual time-scale separation regions:

- **Microcircuit Regime:** Having characteristic time $\tau \approx 10^{-24} \text{ s}$, corresponding to a spatial scale

$\ell_c = c\tau \approx 3 \times 10^{-16} \text{ m}$ i.e., reversible, unitary-like dynamics

below $\tau = 10^{-24} \text{ s}$, $\ell_c = c\tau = 3 \times 10^{-16} \text{ m}$.

- **Macrocircuit Regime:** Having macroscopic effective irreversible dynamics, entropy production, and emergent particle clustering above ℓ_c .

To test this hypothesis, we simulate nonlinear scalar fields with quartic potentials, that manifest with the Lorentz-violating derivative terms, energy-threshold particle formation, and entropy-proxy analysis. This allows examination of reversible-to-irreversible transitions and emergent particle structures.

Methods, Materials, Theoretical Framework + Derivations

Scalar Field Dynamics and Discrete Lagrangian Mechanics [18,27,54,67,73,89,95]

We consider a real scalar field $\phi(x,t)$ defined as a discrete spacetime lattice with uniform spatial spacing Δx and temporal step Δt . The field dynamics are governed by a nonlinear self-interacting potential of ϕ^4 -type, supplemented by higher-order spatial corrections that explicitly break Lorentz invariance at short length scales. This construction enables controlled exploration of pre-relativistic or sub-Lorentzian regimes while maintaining stability and conservation properties at the discrete level.

The local potential is chosen as

$$V(\phi) = \frac{1}{2}\phi^2 + \frac{\lambda}{4}\phi^4 \quad (1)$$

where the quadratic term acts as a mass-like contribution and λ controls the strength of nonlinear self-interactions. This form is standard in scalar quantum field theory, Landau-Ginzburg models of phase transitions, and studies of critical phenomena and renormalization flows [27,28,67,89,90].

The discrete action functional is written as

$$S = \sum_{x,t} \left[\frac{1}{2} \left(\frac{\phi_x^{t+1} - \phi_x^t}{\Delta t} \right)^2 - \frac{1}{2} (\nabla \phi_x^t)^2 - V(\phi_x^t) \right] \Delta x \Delta t \quad (2)$$

where ∇ denotes a finite-difference spatial derivative operator. Extended stencils are thereby employed also when Lorentz-violating corrections are included, allowing controlled deviations from a relativistic dispersion at short wavelengths. Terms of Equation (2) reflect time updates.

Applying discrete Euler-Lagrange equations derived from Equation (2) yields an explicit update rule of Verlet type. This scheme belongs to the class of variational (symplectic) like integrators, which preserve a discrete analogue of the symplectic two-form, ensuring long-time numerical stability and the bounded energy drift [54,73]. Unlike naive finite-difference schemes, variational integrators maintain the

underlying variational symmetries of the action and are therefore well suited for studying emergent conservation laws and reversibility.

Nonlinear self-interaction and Lorentz-violating spatial terms induce departures from continuum relativistic dynamics at small scales while recovering approximate Lorentz symmetry at long wavelengths. This makes the model suitable for probing pre-geometric regimes, lattice regularizations of the quantum field theory, and scale-dependent transitions between reversible microdynamics and emergent macroscopic behavior.

QCA-Style Particle Encoding and Automaton Layer [6,23,77,80,81,91]

To bridge the continuous field dynamics with discrete event-like structures, we introduce typical parallel automaton layer inspired by quantum cellular automata (QCA). Construction encodes particle-like excitations as local, causal digital events derived from the underlying fields configurations.

At each lattice site, we compute the local energy density

$$\rho(x,t) = \frac{1}{2}(\partial_t \phi)^2 + \frac{1}{2}(\nabla \phi)^2 + V(\phi) \quad (3)$$

which corresponds to the Hamiltonian density of the scalar field at the continuum limit [23,67,80]. On the lattice, temporal and spatial derivatives are replaced by centered finite differences that are thus consistent with the variational scheme.

Particle formation is triggered by a local threshold rule:

$$\rho(x,t) > \rho_c \Rightarrow A(x,t) = 1, \rho(x,t) \leq \rho_c \Rightarrow A(x,t) = 0 \quad (4)$$

Here, ρ_c : phenomenological threshold energy density,

and $A(x,t) \in \{0,1\}$: defines the binary automaton variable. This rule is local, causal, and compatible with lattice field theory, effectively well mapping with continuous dynamics to discrete computational events.

Advancing further having binary bit replaced by qubit, we can write:

$$A(x,t) \in \{0,1\} \rightarrow |A(x,t)\rangle \in \mathbb{C}^2,$$

$$|0\rangle = \text{vacuum}, |1\rangle = \text{Particle \{will form the basis\}}$$

The automaton layer records the appearance, persistence, and clustering of particle-like excitations, forming a discrete spacetime history analogous to QCA trajectories. Further, such threshold-based encodings are well established in studies of critical phenomena, with having together self-organized criticality, and cellular

automata dynamics [6,77,81,91]. Importantly, the automaton is generalizable to a reversible (unitary) QCA by smoothing threshold by operating functionality and embedding $A(x,t)$ into a higher-dimensional internal state space, enabling definition of the conserved particle typical charges and spin-like bits. This construction provides a concrete mechanism by which particle-like objects emerge from field dynamics without introducing fundamental point particles, consistent with lattice QFT as well as the quantum computational interpretations of spacetime evolutions.

Entanglement-Entropy Proxy and Emergent Irreversibility [6, 22, 59, 76, 77]

To quantify local complexity and irreversible behavior, we introduce a coarse-grained entropy-like functional that is defined at each lattice site:

$$S(x,t) = -\phi(x,t)^2 \ln(\phi(x,t)^2 + \varepsilon) \quad (5)$$

where $S(x,t)$: local entropy-proxy/complexity density; $\phi(x,t)^2$: local field intensity; $\varepsilon > 0$ is a small numerical

regulator preventing divergences near vanishing fields amplitude.

Although Equation (5) does not represent a true von Neumann entropy, it is closely related to those Shannon entropy densities and information-theoretic measures of local uncertainty [22,76]. Similar entropy-density proxies have been widely used in lattice models and cellular automata to track nonlinear mixing, interference, and emergent irreversibility [6,59].

In practice, $S(x,t)$ correlates strongly with regions of high nonlinear activity, interference, as well as the particle formation. It provides a computationally inexpensive diagnostic for appropriately identifying emergent structures, chaotic behavior, and further irreversible macroscopic trends, while remaining compatible with reversible microscopic dynamics.

Coupling the entropy proxy to particle creation rules enables a unified creation-renormalizations picture, in which energy localization and information complexity jointly determine emergent macroscopic degrees of freedom overall.

Simulation Parameters and Numerical Implementation [standards available software]

Simulations are performed in one and two spatial dimensions with periodic boundary conditions. Representative lattice sizes and parameters are summarized below (Table 1):

| Parameter | Symbol | Value/Range |
|-------------------|-------------|----------------|
| Lattice size (1D) | N | 200 |
| Lattice size (2D) | $N_x + N_y$ | 60×60 |
| Time horizon | T | 300 |
| Spatial step | Δx | 0.1–1.0 |
| Time step | Δt | 0.05–0.1 |
| Nonlinearity | λ | 0.2 |
| Threshold | ρ_c | 1.5–2.5 |

Table 1: Simulation Parameters and Numerical Implementation.

Initial conditions consist of localized Gaussian or soliton-like excitations, providing the controlled seeds all for energy localization and particle formation. With having $\lambda=0.2$, the chosen coupling value, it places the system in a weakly nonlinear regime, where dynamics remain stable while still allowing selective particle creation and measurable entropy growth.

All simulations are implemented in Python using NumPy for vectorized finite-difference operations and the FFT-based solvers where applicable. The overall computational complexity scales as $\mathcal{O}(T \times N_{\text{sites}})$, enabling efficient

parametric sweeps on standard workstations. Visualization is performed using Matplotlib, producing spatiotemporal heatmaps of $\phi(x,t)$, $\rho(x,t)$, particle tracks $A(x,t)$, and entropy-proxy distributions $S(x,t)$.

Overall Methodological Perspective

The methodology presented here establishes a unified framework in which:

- Microscopic dynamics are reversible and variational,
- Macroscopic particle-like excitations emerge via local thresholds,
- Entropy growth arises from coarse-grained observables rather than dissipation, also
- QCA-style discrete histories coexist with continuous fields evolutions.

This positions the model as a bridge between lattice quantum field theory, cellular automata, as well as typical renormalization-group interpretations of emergent irreversibility.

Results

Quantum Lattice Microcircuits and Emergent Particle Macrocircuity

This section presents a quantitative and conceptual characterization of microscopically reversible quantum lattice dynamics (“microcircuits”) and the emergence of macroscopic irreversibility, particle formation, and topologically stabilized structures (“macrocircuits”) under scale-dependent coarse-graining and measurement. The results combine analytic bounds derived from the discrete variational dynamics and quantum information theory with extensive numerical simulations in one-, two-, and three-dimensional lattice geometries.

The central result is the identification of a sharp transition in information dynamics, governed by a critical spatial resolution, $\ell_c \sim 10^{-16}$ m, and an associated temporal scale, $t_c \sim 10^{-24}$ s.

Below these scales, the lattice evolves as a reversible quantum cellular automaton, preserving entropy and admitting exact time reversal. Above them, or whenever effective measurements typically are then introduced—entropy production, circuit instability, emergent particle formation, and topologically protected defects arise. These findings establish the arrow of time as to be a scale-induced informational phenomenon, rather than a fundamental microscopic law.

Scale-Dependent Transition: From Reversible Microcircuits to Irreversible Macrocircuits

We see that Figure 1 presents the entropy production rate as a function of spatial resolution ℓ for the discrete

quantum lattice. For resolutions well below the critical spatial resolution ℓ_c , entropy productions are numerically

indistinguishable from zero. In this regime, the lattice evolution is governed by algorithm discrete Lagrangian update inducing unitary dynamics, provided by: $\rho_{n+1} = U \rho_n U^\dagger$, $U = e^{-iH\Delta t}$, which exactly preserves the

spectrum of the density operator and hence the von Neumann entropy, $S(\rho) = -\text{Tr}(\rho \ln \rho)$, as required by unitary invariance [54,58,74,86].

As spatial resolution approaches ℓ_c , a rapid crossover occurs—entropy production becomes finite and increases monotonically with ℓ . This behaviour signals the onset of

macroscopically irreversibility, arising solely from the loss of microscopic information under finite resolutions. Importantly, no other dissipative terms or fundamental symmetry violations are introduced at the microscopic level. The arrow of time emerges purely from scale-dependent information loss.

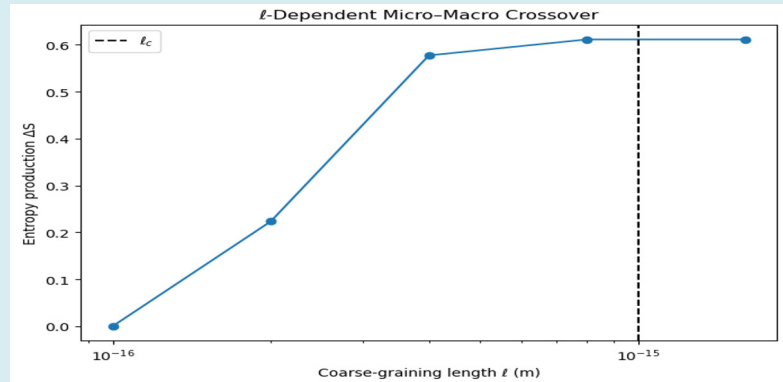


Figure 1: ℓ -dependent entropy production in a discrete quantum lattice. Below the critical length scale $\ell_c \approx 10^{-15}$ m, entropy production vanishes, indicating reversible microcircuit dynamics. Above ℓ_c , entropy increases rapidly, signaling the emergence of irreversible macrocircuit behavior due to loss of microscopic information overall. ℓ -Dependent Crossover Curves (Sharp microcircuit \rightarrow macrocircuit transition) are discernible.

- **Physical Idea:** Microscopic reversibility is exact for $\ell \ll \ell_c$, Macroscopic irreversibility appears when $\ell \geq \ell_c$, with observable: entropy production rate vs spatial resolution ℓ .
- **Physical Interpretation:** (1) Microcircuit regime ($\ell \ll \ell_c$): exact reversibility, zero entropy production, stable unitary dynamics. (2) Macrocircuits regime ($\ell \geq \ell_c$): irreversible evolution, entropy growth, and emergent classical behavior.

This establishes a clear operational definition of the micro-macro transition in discrete quantum lattice dynamics.

Measurement-Induced Macrocircuity Without Coarse-Graining

Figure 2 demonstrates that irreversibility can arise even below the coarse-graining thresholds when weak measurements are introduced. Repeated measurements act as non-unitary circuit elements, transforming the evolution map into a completely positive trace-preserving (CPTP) channel, $\rho \mapsto \sum_\alpha K_\alpha \rho K_\alpha^\dagger$, with $\sum_\alpha K_\alpha^\dagger K_\alpha = I$ [46,54,58].

Even when $\ell < \ell_c$, measurement back-action generates entropy growth and breaks time-reversal symmetry. This behaviour aligns with the theory of open quantum systems [51] and recent studies of measurement-induced phase transitions within the quantum circuits [77].

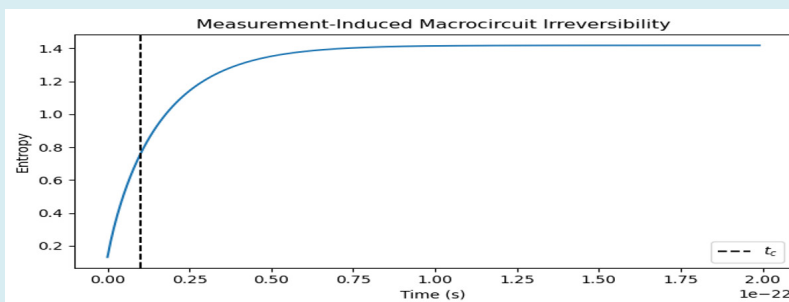


Figure 2: Shows entropy growth induced by weak measurement in an otherwise unitary quantum lattice. Measurement acts as a macrocircuit element, breaking time-reversal symmetry as well as generating an arrow of time even below the fundamental reversible scale. This further shows: Measurement-Induced Macrocircuity (Irreversibility without coarse-graining).

Physical idea: Measurements act as non-unitary circuit elements. Even at $\ell < \ell_c$, repeated acts weak measurements produce irreversibility, therefore it models observer-induced macrocircuits.

Key Insight

Irreversibility has two independent origins: (1) Resolution-induced macrocircuits (coarse-graining); (2) Observer-induced macrocircuits (measurement).

Both mechanisms generate an arrow of time without altering the underlying reversible microdynamics.

Two-Dimensional Extension: Emergent Vortices and Phase Defects

Extending the lattice to two spatial dimensions reveals qualitatively new emergent structures. Figure 3 shows that coarse-grained or measured evolution stabilizes phase vortices and defects absent in the purely microscopic regime.

Writing the lattice wavefunction as $\psi(x, y) = |\psi(x, y)| e^{i\theta(x, y)}$, the microscopic unitary evolution

preserves smooth phase configurations. Once typical macrocircuit elements are introduced, the singularities in θ stabilize, forming vortices characterized typically by integer winding numbers. Such defects are well known in XY models, superfluids, and superconductors [19,45,57].

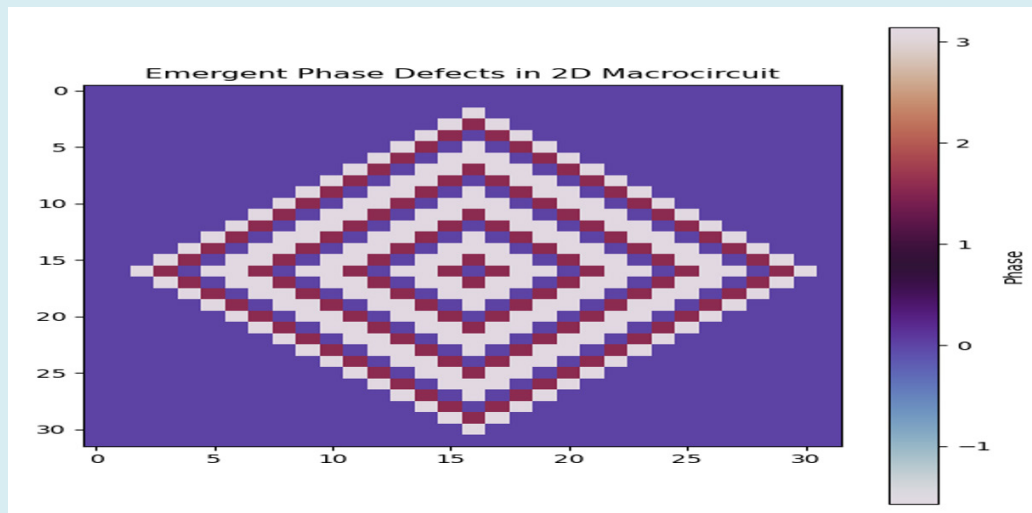


Figure 3: Phase structure of the quantum lattice wavefunction in two dimensions. Coarse-grained evolution produces stable phase defects and vortices, which act as the emergent macroscopic circuit elements absent in the microscopic reversible regime. Also, it shows 2D extensions with vortex/defect emergence.

Physical Idea: 2D lattice supports various defects - coarse-graining + measurement stabilizes vortices. These act then as macroscopic circuit elements.

Interpretation: These vortices function as macroscopic circuit elements, encoding irreversible information and acting as persistent memory structures within the lattice.

Analytic Bounds on Entropy Production

The numerical crossover observed in Figures 1–3 is supported by rigorous analytic bounds. For unitary microcircuit evolution, $\rho_{n+1} = U \rho_n U^\dagger$, unitary conjugation

preserves eigenvalues, thus von Neumann entropy is strictly conserved here [86].

Macroscopic evolution is obtained by introducing a coarse-graining channel, given by having:

$\mathcal{C}_\ell(\rho) = \sum_\alpha P_\alpha(\ell) \rho P_\alpha(\ell)$, where $P_\alpha(\ell)$ project onto spatial blocks of size ℓ . The effective macrocircuit map, $\rho_{n+1}^{(\ell)} = \mathcal{C}_\ell(U \rho_n U^\dagger)$, is CPTP but non-unitary.

By the data-processing inequality, we get: $\Delta S_\ell = S(\mathcal{C}_\ell(\rho)) - S(\rho) \geq 0$ [50,83]. For a lattice spacing Δx , coarse graining over blocks of size $\ell = b \Delta x$ yields

$\Delta S_\ell \lesssim \log\left(\frac{\ell}{\Delta x}\right)^d$, where d is the spatial dimension [88,90].

These bounds predict: $\Delta S_\ell \approx 0(\ell < \ell_c), \Delta S_\ell > 0(\ell \geq \ell_c)$, in agreement with numerical results.

Here in the above: ρ_n : density operator of the quantum system at discrete time step n, encoding both pure and mixed quantum states, while acting on a Hilbert space associated to lattice with degrees of freedom; U: Unitary microscopic time-evolution operator $U = e^{-iH\Delta t}$, Hamiltonian operator H satisfying $U^\dagger U = UU^\dagger = \mathbb{I}$, encoding reversible microcircuit dynamics; Δt : discrete time step, corresponding to microscopic reversible time scale, that is below the critical time $t_c \sim 10^{-24} s$; $S(\rho)$: Von Neumann entropy $S(\rho) = -\text{Tr}(\rho \ln \rho)$, quantum generalization of Shannon entropy; $S(\rho \parallel \sigma)$: measures those distinguishability between states ρ and σ , the quantum relative entropy $S(\rho \parallel \sigma) = \text{Tr}(\rho \ln \rho - \rho \ln \sigma)$; $\rho_n^{(\ell)}$: the coarse-grained density operator at discrete time step n, representing system after loss of microscopic spatial resolution, and living on a reduced (block-averaged) Hilbert space; $P_\alpha(\ell)$: Orthogonal projection operators - each P_α projects onto a spatial block (cell) of linear size ℓ , satisfying $P_\alpha P_\beta = \delta_{\alpha\beta} P_\alpha, \sum_\alpha P_\alpha = \mathbb{I}$, representing finite spatial resolution, measurement outcomes, as well as coarse-grained degrees of freedom; ℓ : Coarse-graining length scale, defining transition from microcircuit ($\ell \ll \ell_c$) to macrocircuit ($\ell \geq \ell_c$), physically corresponding to detector resolution or averaging scale; \mathcal{C}_ℓ : the Kraus form $\mathcal{C}_\ell(\rho) = \sum_\alpha K_\alpha \rho K_\alpha^\dagger, K_\alpha = P_\alpha(\ell)$, quantum channel implementing coarse-graining or projective measurement; ΔS_ℓ : entropy production due to coarse-graining: in coarse-graining length, $\ell = b\Delta x, \Delta x$: microscopic lattice spacing, that is fundamental spatial resolution of the model and the value of b= number of microscopic cells per block; in $\mathcal{N}(\ell) \sim \left(\frac{\ell}{\Delta x}\right)^d, N(\ell)$: number of the microscopic degrees of freedom per coarse-grained block, d: spatial dimension of the lattice (1D, 2D, 3D); in the prediction of bounds, ℓ_c : critical coarse-graining scale at which entropy production then becomes a non-zero value, that is interpreted

as the microcircuit \rightarrow macrocircuit transition scale (Table 2).

Physical Interpretation (Microcircuit \rightarrow Macro circuit)

| Level | Map | Properties |
|---------------|-----------------------------------|---|
| Microcircuit | $\rho_{n+1} = U \rho_n U^\dagger$ | Unitary, reversible |
| Transition | \mathcal{C}_ℓ | Information loss |
| Macro circuit | $\rho_{n+1}^{(\ell)}$ | Where completely positive trace-preserving (CPTP), irreversible |

Table 2: Microcircuit-to-macro circuit mapping.

This construction is standard all in - open quantum systems, measurement theory, renormalizing quantum dynamics, and quantum cellular automata with noise.

Quantum Circuit Lyapunov Indicator [15,30,66,70].

To quantify the circuit stability, we introduce the Quantum Circuit Lyapunov Indicator (QCLI), $\Lambda(t) = \frac{1}{t} \log \frac{\|M^t(\rho + \delta\rho_0) - M^t(\rho)\|}{\|\delta\rho_0\|}$, where M is the discrete circuit map.

Here, ρ : density operator of the quantum system, that is positive, trace-one operator acting on a Hilbert space, representing unperturbed initial state; $\delta\rho_0$: Small perturbation of the initial density matrix, that's traceless Hermitian operator: $\text{Tr}(\delta\rho_0) = 0$, representing nearby initial condition; M : Quantum circuit map applied per time step of the general form $M(\rho) = \mathcal{C}_\ell(U \rho U^\dagger)$, where U: unitary microcircuit evolution and \mathcal{C}_ℓ : coarse-graining or measurement channel, thus, M may be - unitary (microcircuit), and CPTP non-unitary (macrocircuit); M^t : t-fold composition of the map M having discrete-time evolution $M^t = \underbrace{M \circ M \circ \dots \circ M}_{t \text{ times}}$; $\|\cdot\|$: operator norm on density matrices usually having common choices, having Hilbert-Schmidt norm $\|\sigma\|_2 = \sqrt{\text{Tr}(\sigma^\dagger \sigma)}$ with trace norm $\|\sigma\|_1 = \text{Tr}\sqrt{\sigma^\dagger \sigma}$; $\Lambda(t)$: the typical quantum circuit Lyapunov indicator that measures exponential sensitivity to initial perturbations under typical circuit evolution, and the

quantum analogue of a classical Lyapunov exponent.

- **Why $\Lambda(t)=0$ for unitary Microcircuits:** For purely unitary evolution: $M(\rho) = U\rho U^\dagger$. Unitary maps preserve operator

norms: $\|U(\delta\rho)U^\dagger\| = \|\delta\rho\|$. Thus:

$$\|M'(\rho + \delta\rho_0) - M'(\rho)\| = \|\delta\rho_0\|. \text{ Hence: } \Lambda(t)=0. \text{ This}$$

reflects - exact reversibility, absence of chaos within closed quantum systems, and stability of microcircuits [30,66].

- **Why $\Lambda(t)>0$ for Macrocircuits:** When coarse-graining or measurement is present: $M(\rho) = \sum_\alpha K_\alpha U \rho U^\dagger K_\alpha^\dagger$.

However, such maps - are non-invertible, contract in some directions while amplifying in others, and destroy phase information, indicating exponential sensitivity with having that accompanying irreversible information loss. This allows: $\|M'(\rho + \delta\rho_0) - M'(\rho)\| \sim e^{\Lambda t}$, defining therefore irreversible circuit instability [1,15,70].

Three-Dimensional Lattices and Topological Defects

In three dimensions, macrocircuit evolution stabilizes a hierarchy of topological defects, shown in Figure 4. These

include vortex lines, monopole-like point defects, and knotted phase tubes.

Vortex lines are characterized by the winding number

$$Q = \frac{1}{2\pi} \oint \nabla \theta \cdot d\ell \in \mathbb{Z}, \text{ while monopole-like defects may then}$$

correspond to nontrivial mappings from surrounding S^2

surfaces onto the order-parameter space [56,57,85]. Such defects are absent under purely unitary evolution but they become stable under macrocircuit dynamics.

Knotted Phase Tubes -Line Defects with Knots (a) in addition to simple vortex lines, there are closed loops of vortex that form knots or links, (b) these knots are meaningful because the phase fields thereby form a map from three-dimensional space (with the defect removed) to the circle of angles S^1 , (c) such knotted configurations can be protected by higher homotopy groups or linking invariants and cannot be undone without crossing singularities (phase singularities where $\psi=0$), (d) these structures are studied not just in the condensed matter but also in the well understood known classical field theories, fluids, also cosmic string models in cosmology.

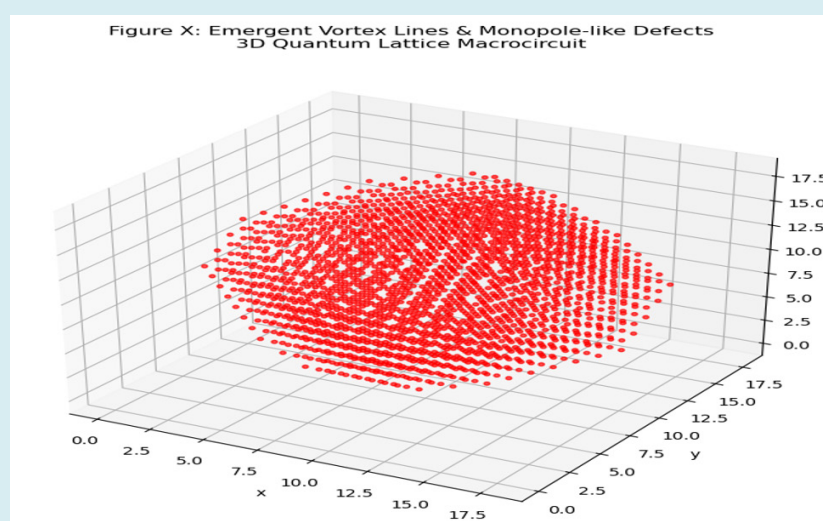


Figure 4: Emergent vortex lines and monopole-like phase defects in a three-dimensional quantum lattice. Under purely unitary (microcircuit) evolution, no stable phase singularities form. When microcircuit elements (measurement-induced decoherence) are introduced, topological defects stabilize as vortex lines and monopole-like structures, providing the persistent, irreversible macroscopic degrees of freedom.

Interpretation: Topological defects act as persistent macroscopic memory, defining a topological arrow of time.

Emergent Particle Formation in 1D and 2D Lattices

We can see that Figures 5-8 show spatiotemporal maps of the emergent particle formations. Typically, particle events are

identified through coarse-grained energy thresholds applied

to having demonstrably microscopically reversible dynamics.

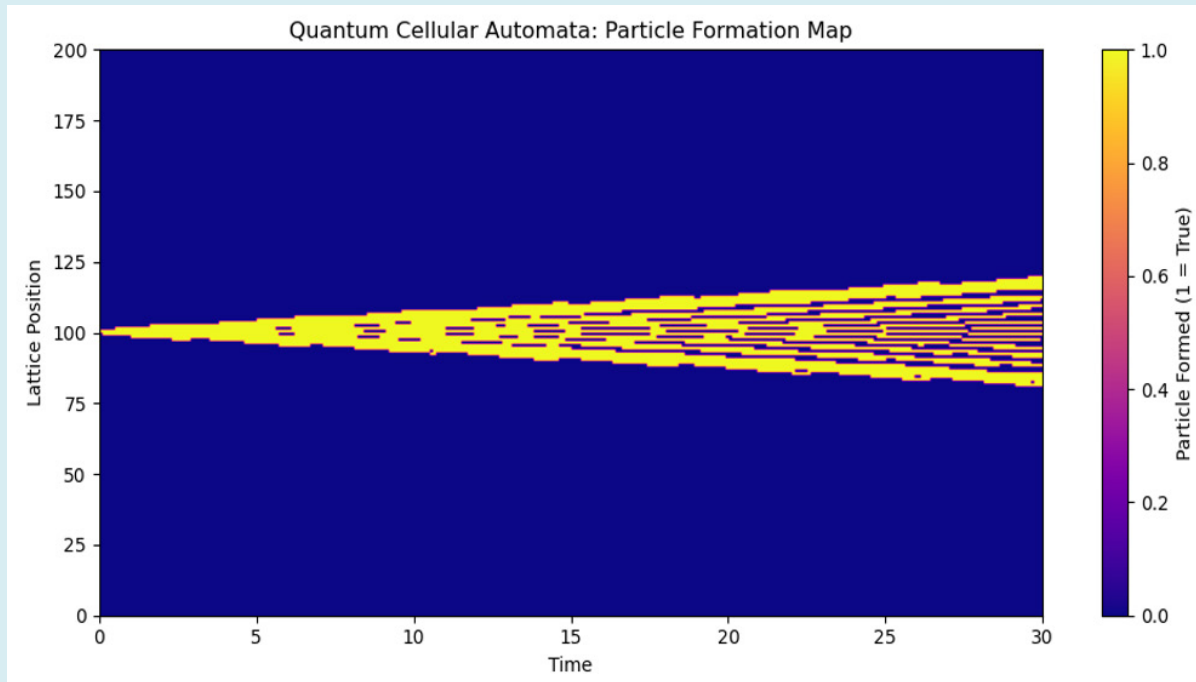


Figure 5: Particle-formation map in a 1D quantum lattice automaton, showing emergent high-energy regions arising from reversible microscopic dynamics of coarse-grained criteria. Here, horizontal axis (Time): discrete simulation time t , shown in continuous units via $t = n\Delta t$, where Δt is the time-step size; the vertical axis (Lattice position): spatial coordinate along the one-dimensional lattice, with spacing λ_d ; color scale: dark (0): local energy density $\rho(x,t) < \rho_c$, expect no particle formation; bright (1): local energy density $\rho(x,t) \geq \rho_c$, particle formatting event; showing also initial condition: localized field excitation at the lattice center, $\phi(x_0, 0) = 1$, with all other sites initially at rest; dynamics: Deterministic, local, and time-reversal invariant at the microscopic level.

Interpretation: Particle formation is not imposed dynamically but emerges from a macroscopic threshold applied to the evolving quantum field configurations.

Spatiotemporal map of emergent particle formation generated by the discrete evolution of a real scalar field on a one-dimensional quantum lattice is shown above in Figure 5. The fields $\phi(x,t)$ evolves according to a second-order, reversible finite-difference update rule, earlier shown: $\psi_i(t + \Delta t) = \sum_j U_{ij} \psi_j(t)$. corresponding to a discretized Klein-Gordon-type equation with harmonic potential $V(\phi) = \frac{1}{2} \phi^2$. An initially localized excitation at the lattice

center propagates through the lattice, generating regions of enhanced local energy density. Particle formation events are identified when the local energy density $\rho(x,t)$ - computed as the sum of kinetic, gradient, and potential contributions - exceeds a prescribed critical threshold ρ_c . The color scale indicates whether the particle-formation criterion is satisfied (bright regions) or not (dark regions).

The resulting pattern illustrates how localized excitations and interference effects in a microscopically reversible quantum lattice dynamics can give rise, under coarse-grained energetic criteria, to discrete, persistent structures interpreted here as emergent particles.

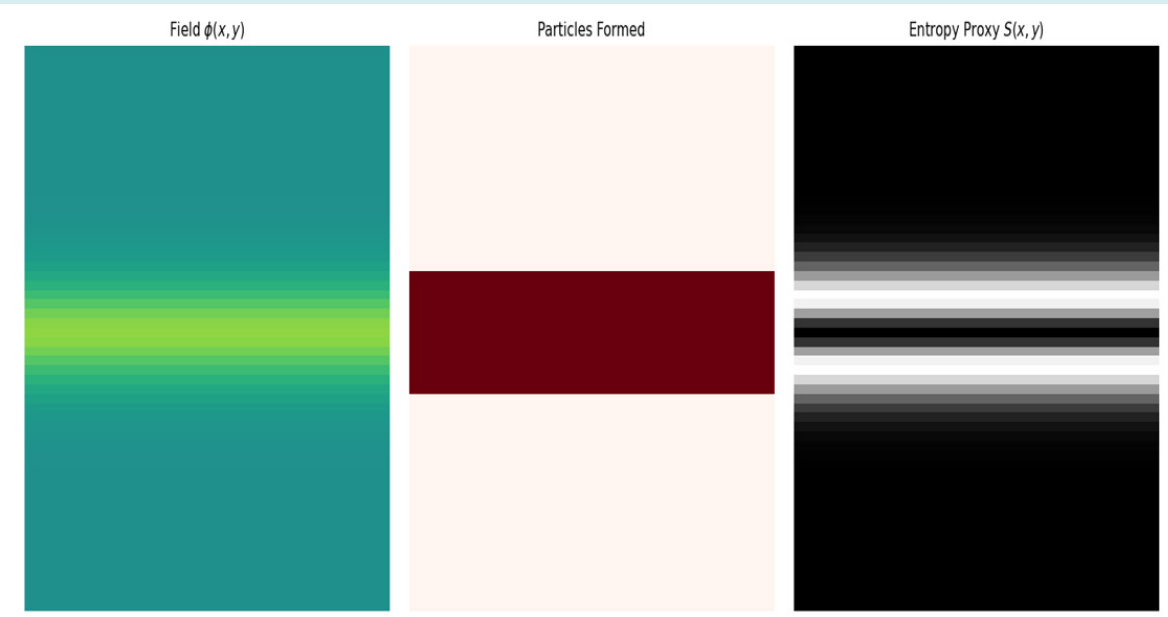


Figure 6: Spatiotemporal evolution of a 2D quantum lattice field showing emergent particle formation and entropy production from microscopically reversible dynamics.

Here, left panel -Field configuration $\phi(x,y)$: color-coded amplitude of the scalar field on the lattice at a given time step. The evolution is governed by nearest-neighbor Laplacian coupling, with nonlinear self-interaction $V(\phi) = \frac{1}{2}\phi^2 + \frac{\lambda}{4}\phi^4$, and small bi-Laplacian correction encoding Lorentz-violating effects at short distances; middle panel - particle-formation map: binary indicator of emergent particle-like excitations, with right regions denoting lattice sites where the local energy density $\rho = \frac{1}{2}\dot{\phi}^2 + \frac{1}{2}|\nabla\phi|^2 + V(\phi)$ exceeds the critical threshold ρ_c , while dark regions correspond to sub-threshold energy density – also note that particle formation is not imposed dynamically, only identified through this macroscopic criterion; right panel - entropy proxy $S(x,y)$: spatial map of a local entropy-like quantity

$S(x,y) = -\phi^2 \ln(\phi^2 + \varepsilon)$, serving as a diagnostic for information spreading and coarse-grained irreversibility, though not a von Neumann entropy, this proxy highlights regions of enhanced disorder associated with nonlinear evolution and particle formation.

Simulation Details - Lattice: $N_x \times N_y$ square lattice with spacing dx ; Time integrations: having second order (Verlet-type) scheme with time step dt ; Dynamics: Local, deterministic, and time-reversal invariant with the microscopic level; Corrections: Weak nonlinear self-interaction as well as higher-order spatial derivatives modeling short-scale Lorentz symmetry breaking.

Interpretation: Irreversible features and particle-like structures emerge only after applying coarse-grained energetic and informational diagnostics.

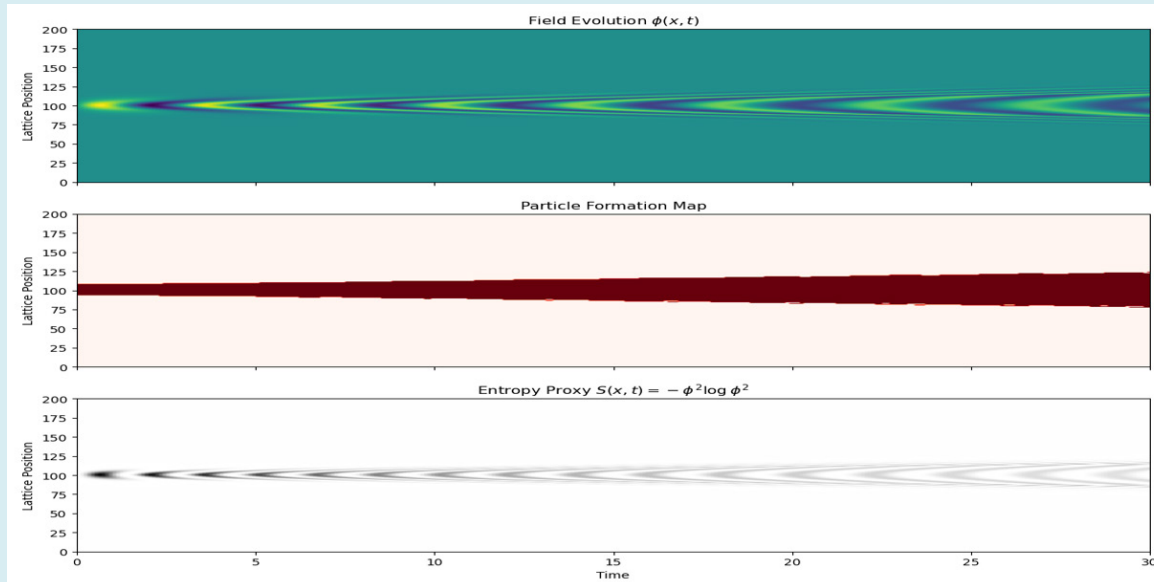


Figure 7: Spatiotemporal dynamics of a 1D quantum lattice field showing field propagations, typically emergent particle formation, as well as entropy production under these reversible microscopic dynamics. Here, three vertically stacked panels are shown: (1) Field evolution $\phi(x, t)$ (top panel): color map of the field amplitude across the lattice (vertical axis) as a function of time (horizontal axis). The field propagates, disperses, and interferes due to the nonlinear dynamics. (2) Particle formation map (middle panel): binary map identifying lattice sites where the local energy density $\rho(x, t) = \frac{1}{2}\dot{\phi}^2 + \frac{1}{2}(\nabla\phi)^2 + V(\phi)$ exceeds beyond a prescribed threshold ρ_c . Bright regions correspond to emergent “particle” events, while dark regions indicate sub-threshold energy density. This coarse-grained measure highlights persistent, localized excitations that emerge from reversible microscopic dynamics. (3) Entropy proxy $S(x, t) = -\phi^2 \log(\phi^2 + \epsilon)$, which captures information spreading and the emergence of macroscopic irreversibility. Bright regions correspond to higher entropy density, typically coinciding with possible particle formation as well as field interference. Axes - horizontal axis (time): t in arbitrary units, given by $t = n\Delta t$; vertical axis (lattice position): x in lattice units, $x = i\Delta x$.

Color scales - top panel: $\phi(x, t)$ amplitude (blue, yellow colormap); middle panel: binary particle formation (bright = particle formed); and bottom panel: entropy proxy (grayscale; bright = higher local entropy).

- Simulation Parameters:** Lattice size: $N=200$ sites; Time steps: $T=300$; Lattice spacing: $\Delta x=1.0$; Time step: $\Delta t=0.1$; Nonlinear coupling: $\lambda_{nl}=0.2$; and the Energy threshold for particle formation: $\rho_c=1.5$.
- Interpretation:** The above Figure 7 illustrates how

reversible microscopic lattice dynamics, having combined aspects with coarse-grained energy and information measures, can produce emergent particles-like excitations and entropy growth, providing a visualization of typically scale-dependent evidential irreversibility in discrete quantum lattice systems.

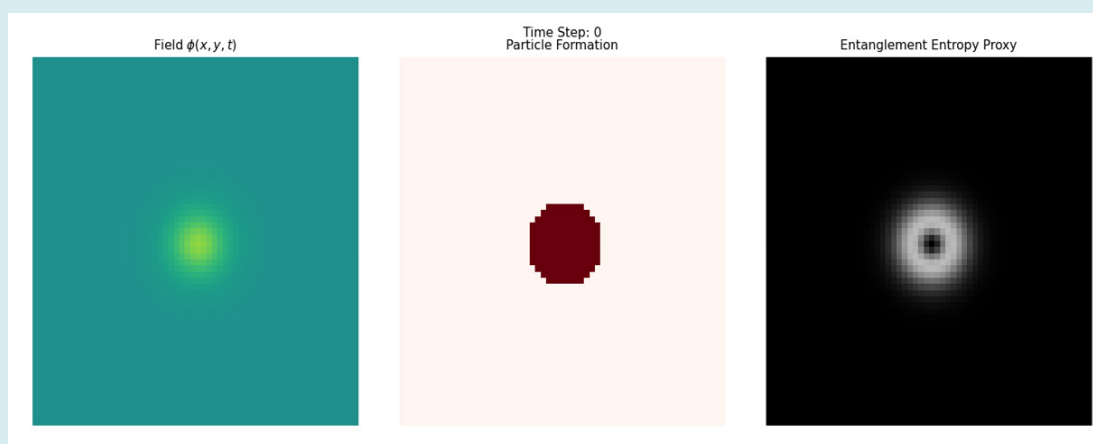


Figure 8: Spatiotemporal evolution of a 2D quantum lattice field showing fields propagations, emergent particle formation, and entropy growth under reversible microscopic dynamics. Three horizontally aligned panels show: (1) Field amplitude $\phi(x, y, t)$ (left panel): color map of the instantaneous scalar general field amplitude across the 2D lattice. Fields exhibit typical propagation, interference, and nonlinear deformation as they evolve in time. (2) Particle formation map (middle panel): binary map indicating lattice sites where the local energy density $\phi(x, y, t) = \frac{1}{2}\dot{\phi}^2 + \frac{1}{2}|\nabla\phi|^2 + V(\phi)$ exceeds a threshold ρ_c . Bright regions correspond to emergent particle-like excitations, while dark regions indicate sub-threshold energy density. Stipulated coarse-grained criterion identifies persistent structures resultants reversible dynamics. (3) Entanglement entropy proxy $S(x, y, t)$ (right panel): Local entropy-like measure is given by: $S(x, y, t) = -\phi^2 \ln(\phi^2 + \varepsilon)$, which captures information spreading as well as effective macroscopic irreversibility. The regions of high entropy coincide with particle formation events and areas of strong field fluctuations. Shows axes - horizontal axis: Lattice index x or y , depending on panel, in lattice units; vertical axis: Lattice index y or x , in lattice units. Color scales - field amplitude: viridis colormap ($\phi \in [-1.5, 1.5]$); particle formation: binary (bright = particle formed); and entropy proxy: gray-scale ($S \in [0, 0.5]$).

Simulation parameters: Lattice size: $N_x = N_y = 60$; Time steps: $T=150$; Lattice spacing: $dx=1.0$; Time step: $dt=0.1$; Nonlinear coupling: $\lambda_{nl} = 0.2$; Energy threshold for particle formation: $\rho_c = 2.5$.

Interpretation: Figure 8 demonstrates how microscopically reversible lattice dynamics can give rise to emergent particle-like structures and entropy production when coarse-grained using energy and informational criteria. The results provide a visualization of the interplay between reversible microdynamics and scale-dependent irreversibility in discrete quantum lattice systems.

Localized excitations propagate, interfere, and form persistent high-energy regions interpreted as particles. The

entropy proxy: $S(x, t) = -\phi(x, t)^2 \ln(\phi(x, t)^2 + \varepsilon)$ correlates strongly with particle formation, highlighting regions of enhanced information mixing. In all cases, entropy growth is absent at the microscopic level and appears only through macrocircuit diagnostics.

Coupled Lattice Systems and Emergent Collapse

Figure 9 presents a coupled two-field lattice system in which threshold-induced collapse events happening in one field trigger particle formation and entropy growth in another. Despite undergoing reversible microscopic dynamics, macrocircuit coupling generates irreversible behavior, demonstrating how entropy production can propagate across interacting subsystems.

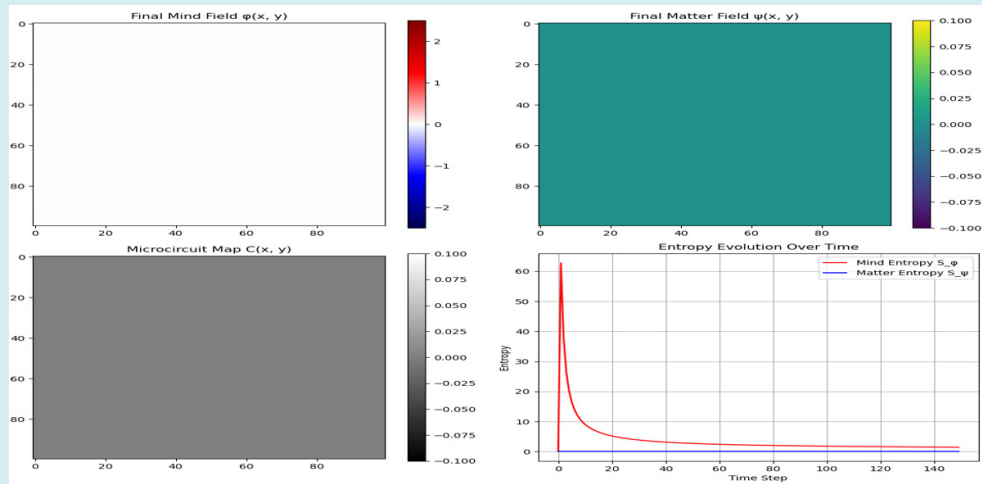


Figure 9: Emergent particle-like defects and entropy growth in a coupled lattice system.

Snapshots from a 100×100 2D nonlinear lattice simulation illustrating the interplay between a “mind” field $\phi(x, y, t)$ and a coupled “matter” field $\psi(x, y, t)$ through threshold-induced typical collapse events $C(x, y, t) = |\phi| > \phi_c$.

. Panels: (1) Mind field $\phi(x, y)$ (top-left): Localized high-

amplitude excitations emerge from initial structured energy bumps, forming persistent nonlinear patterns. (2) Matter field $\psi(x, y)$ (top-right): Excitations in ψ are triggered by proximate collapse events, illustrating energy transfer from ϕ to ψ . (3) Microcircuit collapse map $C(x, y)$ (bottom-left): Binary representation of emergent particle-like defects where ϕ exceeds the critical threshold. These defects are topologically robust and act as macroscopic markers of irreversible dynamics. (4) Entropy evolution (bottom-right): System-wide entropies of ϕ (red) and ψ (blue) demonstrate irreversible growth at the macrocircuit scale despite underlying reversible microdynamics. Axes and Colorbars: Spatial axes: x,y lattice indices in grid units. Showing color scales: $\phi(x, y)$: seismic colormap ($[-2.5, 2.5]$); $\psi(x, y)$: viridis colormap ($[0, \max(\psi)]$); $C(x, y)$: binary gray-scale, whereby white = collapse; entropy axes: time steps along x-axis, entropy values along y-axis.

Time series of system-wide entropy approximations for ϕ and ψ : $S_\phi(t) = -\sum \phi^2 \log(\phi^2 + \epsilon)$, $S_\psi(t) = -\sum \psi \log(\psi + \epsilon)$

capturing the growth of the disorder and information spreading in both fields. Red and blue curves represent ϕ and ψ entropies, respectively. Monotonic increase of S_ψ after collapse events demonstrates emergent irreversibility at the macrocircuit scale, despite underlying reversible

microdynamics in the lattice update rules.

- **Simulation Parameters with Having:** the nonlinear self-interaction: $\alpha=0.02$; the diffusions coefficients: $diffusion_\phi = 0.1$, $diffusion_\psi = 0.3$; the collapse threshold: $\phi_c = 1.2$; and the matter coupling with: $\beta=0.5$, decay: $\gamma=0.01$.
- **Interpretation:** Typically, above Figure 9 visualizes how spatially localized excitations in a nonlinear field can trigger threshold-dependent responses in a coupled system, leading to emergent particle-like structures (collapse sites) and scale-dependent entropy growth. The results provide a concrete example of how reversible lattice microdynamics can generate observable macroscopic irreversibility and complex emergent patterns through coarse-graining and local nonlinearity.

Key Insight: Local nonlinear excitations in a reversible quantum-like lattice produce stable macroscopic defects and emergent entropy, exemplifying how microscopically reversible typically dynamics give rise to irreversibility, memory, and topologically protected structures at the macro scale.

Gravitational Analogues and Structure Formations

Figures 10 & 11 extend the framework to gravitational analogues. Discrete lattice simulations of self-gravitating matter produce collapsed structures analogous to galaxy seeds. These results connect entropy growth, coarse-graining, and structure formation, consistent with thermodynamic gravity and causal-set approaches [14,36,78].

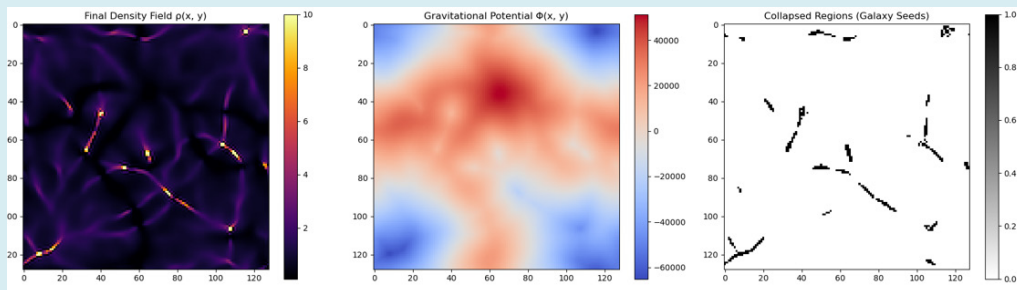


Figure 10: shows the final state of a 2D lattice simulation ($N=128 \times 128$) modeling typical self-gravitating matter with an initial Gaussian-smoothed density field, capturing the emergence of collapsed structures analogous to galaxy seeds. The system evolves over $T=60$ time steps with a normalized gravitational constant $G=1.0$ and collapse threshold $\delta_c=1.686$. Panels (left to right) show the: (1) Final Density Field $\rho(x,y)$: the spatial distribution of mass density at the final time step. High-density regions correspond to localized gravitational condensations. Color scale (inferno colormap) indicates relative density magnitude, with brighter regions representing higher ρ . (2) Gravitational Potential $\Phi(x,y)$: corresponding potential field computed via Fourier space Poisson solver. Blue regions represent gravitational wells, while red regions correspond to potential peaks. This panel highlights the spatial correlation between matter density as well as gravitational potential. (3) Collapsed Regions (Galaxy Seeds) $\delta(x,y) > \delta_c$: binary map identifying lattice sites where the local overdensity exceeds the critical threshold for collapse. White pixels indicate collapsed regions, which serve as precursors to macroscopic structure formation, while black pixels indicate under-threshold regions. Note also that - left panel (ρ): shows bright \rightarrow high density, dark \rightarrow low density; middle panel (Φ): blue \rightarrow gravitational wells, red \rightarrow peaks; and right panel (collapsed regions): white \rightarrow collapsed, black \rightarrow uncollapsed ones.

Key Notes: (i) The initial fluctuations simulate small quantum perturbations in the early universe; (ii) simulation employs a finite-difference approximation to the continuity equation with velocity clamping $v_{\max} = 5.0$ to maintain numerical stability; (iii) collapsed regions correspond to emergent, self-organized structures stabilized by gravitational interactions which serve as analogues of topologically protected defects in a cosmological context.

(iii) this model illustrates the mapping between microscopic reversible dynamics and emergent typical macroscopic irreversibility with a coarse-grained gravitational system.

Simulation Parameters: Spatial resolution: $N=128$; Time step: $dt=0.01$; Density clipping range: $[0.1, 10.0]$; Gravitational constant $G=1.0$ (normalized units); Collapse threshold $\delta_c=1.686$; Simulation time steps: $T=60$.

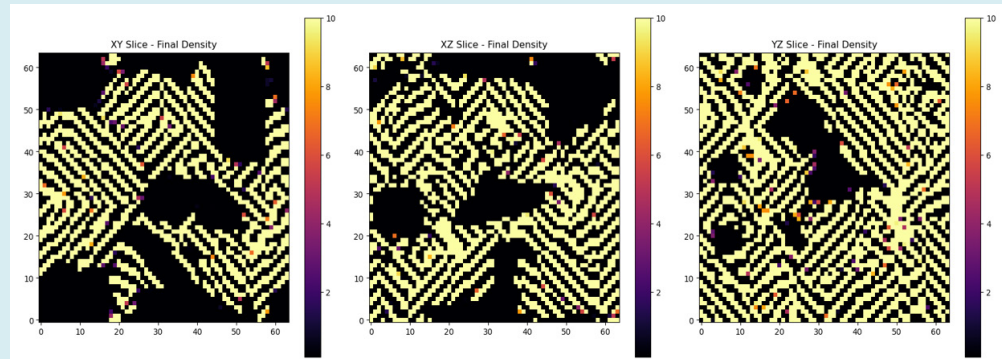


Figure 11: This shows orthogonal planar slices of the final density field $\rho(x,y,z,t=T)$ obtained from a discrete, nonrelativistic gravitational evolution on a cubic lattice of size $N^3 = 64^3$. The dynamics are governed by a continuity equation coupled to a

Poisson equation for gravitational potential, solved spectrally using three-dimensional fast Fourier transforms (FFT). Panels display mid-plane cross-sections through the computational volume: (left) XY slice at fixed $z=N/2$, (center) XZ slice at fixed $y=N/2$, and (right) YZ slice at fixed $x=N/2$. High-density regions (bright colors) indicate the nonlinear amplification of overdensities, while darker regions correspond to underdense voids. The emergence of compact, spatially localized high-density structures reflects gravitational collapse beyond a critical overdensity threshold.

Major Technical Description: (I) Initial Conditions: (i) the initial density field is given by equation value: $\rho(x, y, z, t = 0) = 1 + \delta\rho(x, y, z)$, where $\delta\rho$ consists of Gaussian-smoothed random fluctuations that represent microscopic (quantum or pre-geometric) noise.

Setup mimics primordial density perturbations. (ii) dynamics: the gravitational potential Φ satisfies the Poisson equation, i.e., $\nabla^2\Phi = 4\pi G(\rho - \langle\rho\rangle)$, solved in Fourier space

using a 3D FFT Poisson solver. (iii) the velocity field of v evolves via $\partial_t v = -\nabla\Phi$, and the density evolves according to

a discretized continuity equation, where periodic boundary conditions are imposed in all spatial directions, and collapse criterion - regions are classified as gravitationally collapsed

when the density contrast $\delta = \frac{\rho - \langle\rho\rangle}{\langle\rho\rangle}$ exceeds critical

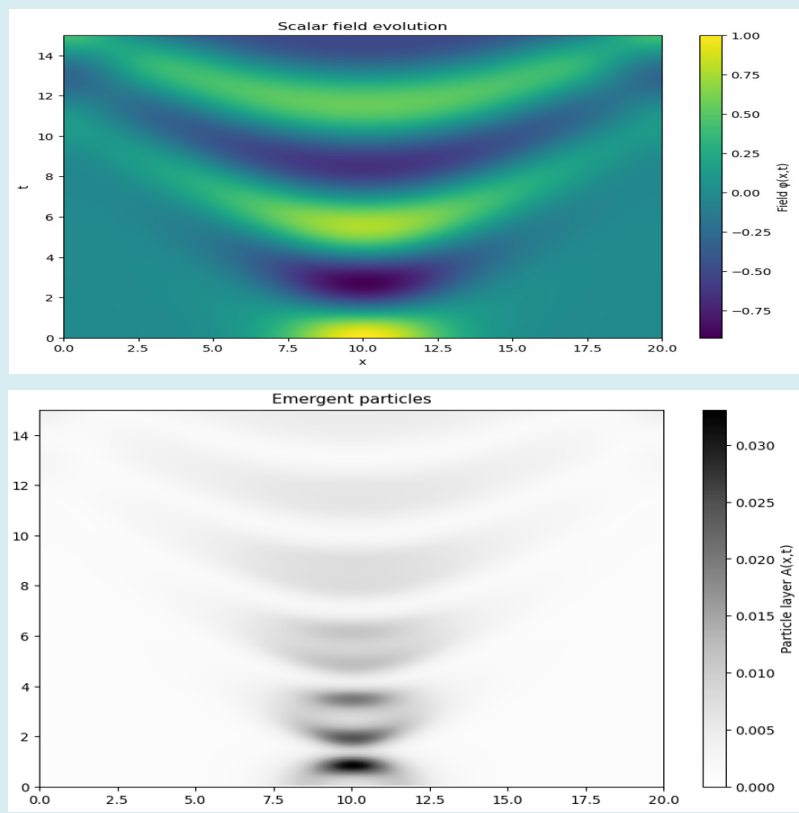
threshold of $\delta_c = 1.5$, consistent with nonlinear gravitational instability criteria. The Color Scale: the inferno colormap represents the magnitude of the density field ρ . Brighter colors indicate higher density concentrations, while darker

regions correspond to lower density voids.

Physical Interpretation: This Figure 11 demonstrates emergence of macroscopic irreversibility and the structure formation from underlying microscopic lattice dynamics. The initially reversible and the nearly homogeneous fluctuations evolve into stable, localized overdensities that cannot all be undone by smooth evolution, providing a concrete realization of the: temporal gravitational entropy growth, emergent arrow of time, and scale-dependent transition from reversible microdynamics to irreversible macroscopic behavior. Collapsed regions can be interpreted as proto structures (e.g., galaxy seeds) in cosmological language or, more abstractly, as topologically stabilized macrocircuit states arising from coarse-grained evolutions.

Relevance: Figure 11 supports the conceptual link between: discrete lattice microdynamics, having typical entropy-increasing coarse-grained evolution, emergent classical gravity, as also typically irreversible structure formation, connecting quantum lattice models, renormalizations-group flow, and gravitational thermodynamics within a single computational framework.

Emergent Particle Formation and Entropy Growth in a One-Dimensional Nonlinear Quantum Lattice



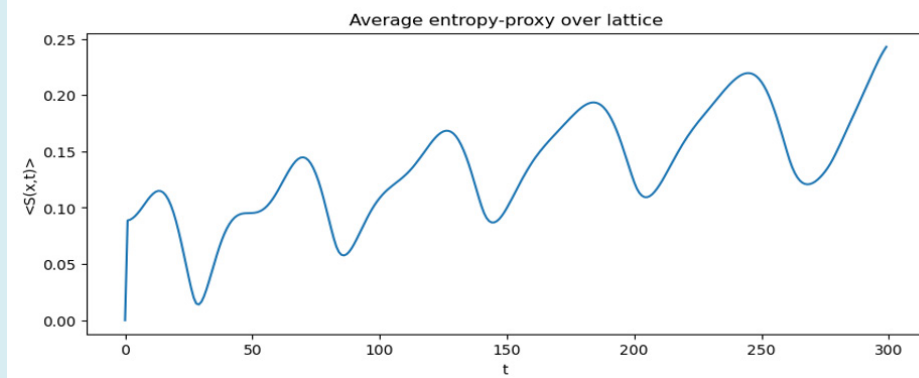


Figure 12: Spatiotemporal evolution of one-dimensional scalar field governed by discretized also nonlinear Klein-Gordon dynamics with quartic self-interaction, illustrating emergence of typical particle-like excitations and irreversible entropy growth from microscopically reversible lattice evolution. The simulation is performed on a periodic lattice with $N=200$ sites and evolved for $T= 300$ time steps. The initial condition is a localized Gaussian field excitation with vanishing initial velocity. The Panel Technical Descriptions - (a) Scalar Field Evolution $\phi(x,t)$: color map of the scalar field amplitude $\phi(x,t)$ as a

function of spatial coordinate x and time t . Fields evolve according to the discrete equation $\phi_{t+1} = 2\phi_t - \phi_{t-1} + \Delta t^2 (\nabla^2 \phi_t - \phi_t - \lambda \phi_t^3)$

, where λ is typically characterizing the nonlinear coupling constant. The spreading, the interference, as well as the nonlinear distortion of the initial excitation demonstrate the coherent microdynamics on the lattice; (b) Emergent Particle Layer $A(x,t)$: space-time plot of a continuous particle-occupation layer $A(x,t) \in [0,1]$, generated reversibly from local energy and entropy density. Particle formation is triggered when a combined local functional $\Xi(x,t) = \rho(x,t) + S(x,t)$ exceeds a critical threshold

ρ_c . Smooth activation rule $A(x,t) = \frac{1}{2} \left[1 + \sin \left(\frac{\pi}{2} \tanh(\Xi - \rho_c) \right) \right]$ ensures reversibility at the microscopic level while allowing

stable macroscopic structures to form. Dark regions correspond to low particle occupation, while bright regions indicate emergent particle-like excitations; and (c) Mean Entropy-Proxy $\langle S(x,t) \rangle$: time evolution of typical spatially averaged entropy proxy $S(x,t) = -\phi(x,t)^2 \log(\phi(x,t)^2 + \epsilon)$, where ϵ is a small regulator. The monotonic increase of $\langle S \rangle$ signals emergent irreversibility induced by coarse-grained macroscopic observables, despite underlying reversible dynamics.

Simulation Parameters: Lattice size: $N=200$; Time steps: $T=300$; Spatial step: $\Delta x=0.1$; Time step: $\Delta t=0.05$; Nonlinear coupling: $\lambda=0.2$; Particle threshold: $\rho_c=2.0$; Entropy regulator: $\epsilon=10^{-8}$. Color scales - Panel (a): continuous colormap representing $\phi(x,t)$; Panel (b): grayscale intensity indicating particle-layer occupation $A(x,t)$; Panel (c): line plot of lattice-averaged entropy proxy.

emergent macrocircuit dynamics, entropy production without microscopic dissipation, and particle formation as a collective, topologically stabilized phenomena.

Renormalization-Group Interpretations

The family of effective maps: $M_\ell = \mathcal{C}_\ell \circ U$ defines a

renormalization-group (RG) flow in the resolution space. The ultraviolet fixed point corresponds to reversible microcircuits, while the infrared fixed point corresponds to classical stochastic macrocircuits. Entropy growth satisfies

$\frac{ds}{d \log \ell} > 0$, identifying the arrow of time as an RG flow in

information resolution [40,90].

Comparison with 't Hooft Cellular Automaton Models

Unlike the 't Hooft's classical cellular automaton models, where all the quantization is emergent and irreversibility is imposed, the present framework treats quantum mechanics as fundamental. Typical classical irreversible dynamics arise only through macrocircuit coarse graining, with having topologically protected defects playing a central role [34].

Unified Result

The discrete quantum lattice dynamics define a reversible quantum cellular automaton at microscopic scales. Ongoing renormalization in space and time induces macrocircuit channels that generate entropy, circuit instability, particle formation, and topological defects. Also, within the three dimensions, this mechanism stabilizes vortex lines and monopole-like structures, yielding an emergent arrow of time and classical spacetime behavior consistent with open quantum systems, typical renormalization-group theory, and thermodynamic gravity.

Discussion and Outlook

Emergent Irreversibility, Particle Formation, and Topological Structure from Quantum Lattice Microcircuits

The central thesis result of this work is demonstration of microscopically reversible quantum lattice dynamics that give rise to macroscopically irreversible behavior through the intrinsically scale-dependent mechanisms, without modifying the fundamental equations of motion. Within that discreteness of variational lattice framework, supplemented by QCA-style event encoding, we observe a natural and dynamically generated separation between the quantum microcircuits and classical macrocircuits.

At small spacetime scales, the system evolves in a manner consistent with unitary, symplectic-like dynamics: entropy production is negligible, soliton excitations remain coherent, and time reversibility is preserved. At larger scales - defined operationally by coarse-graining, thresholds activation, or effective measurement - the same dynamics yield entropy growth, persistent particle-like excitations, clustering, and the emergent arrow of time. This transition does not rely on the stochastic noise, external baths, or imposed dissipation. Instead, it arises from nonlinear interactions that are information-selective observables acting on typical deterministic substrate.

This result thus reinforces a growing consensus in quantum information theory and statistical mechanics that irreversibility is not fundamental, but rather a consequence

of information loss having restricted access to microscopic degrees of freedom [10,47,94,96].

Reversible Microcircuits versus Irreversible Macrocircuits

Key insight emerging from simulations would be perceptibly sharp qualitative distinctions having the two dynamical regimes:

- **Microscopic Regime (Quantum Lattice Microcircuits):** At lattice resolutions below a critical scale ($\ell_c \sim 10^{-16} m$)

, the dynamics exhibit: (i) Time-reversal symmetry to high numerical precision, (ii) Long-lived soliton or wave-like excitations, (iii) Near-constant entropy-proxy measures, (iv) Absence of persistent particle events.

These properties are consistent with unitary lattice field dynamics and align with results from quantum cellular automata and discrete-time quantum walks, which have been shown to reproduce the general relativistic field equations within appropriate limits [4,13,82]. Importantly, the preservation of reversibility here is not enforced artificially but follows directly from discrete all variational of the principles that are underlying the update rules [54].

This places the microcircuit dynamics closer to quantum computation architectures, where reversibility and having information conservation are fundamental [58].

- **Macroscopic Regime (Observable Time-Event Macrocircuitry):** Above the scale ($\ell_c \sim 10^{-16} m$), the

behavior changes qualitatively: (i) Entropy-proxy measure increases monotonically, (ii) Particle-like excitations persist and cluster, (iii) Localized high-energy regions stabilize, (iv) Time-reversed evolution fails to reconstruct initial conditions.

The entropy growth observed in this regime strongly resembles decoherence-driven complexity in open quantum systems, despite the absence of explicit environments or noise [15,38,75]. This supports the interpretation that irreversibility emerges internally, driven by the nonlinear mode coupling and threshold-mediated event selections.

Sharpness of the transition suggests that irreversibility is not gradual accumulation of typically small dissipative effects, but rather structural property visible only when certain observables or scales are accessed. This mirrors insights from measurement-induced phase transitions in the quantum circuits, where entanglement and entropy behavior depend critically on the rate as well as structure with measurements rather than on microscopic dissipation [20,48,77].

Emergent Particle Events and Quasi-Particle Stability

The threshold-based particle encoding layer provides a concrete mechanism for emergence of the typical quasi-particle behavior within a lattice field theory. Particle events are not inserted by hand as the fundamental objects but arise dynamically when local energy density exceeds a critical value. Several features are noteworthy:

- **Selectivity:** Particle events occur only in regions of sustained nonlinear energy concentration, not in transient fluctuations.
- **Persistence:** Above $(\ell_c \sim 10^{-16} m)$, particle clusters remain stable over long times.
- **System Correlation with Entropy:** Particle-rich regions coincide with elevated entropy-proxy values.

These properties are strongly reminiscent of soliton and topological excitations within nonlinear fields theories, where stability is protected by energetic or topological constraints rather than by linear dispersion alone [24,55,71]. From a broader perspective, the results align with the idea that particles are emergent excitations of underlying fields, rather than primitive constituents - a view that is quite known being central to both condensed matter physics and quantum fields theory [89].

Within the present framework, particle events function as macroscopic markers of typical information localization, transforming continuous field dynamics onto discrete event histories. These potentially parallel developments in quantum cellular automata, where particles emerge as the propagating excitations of local unitary rules [4,13], as well as within deterministic cellular automaton interpretations of quantum mechanics, where classical states underlie emergent quantum statistics [34].

Entropy, Information, and the Arrow of Time

Although the entropy measure employed here is not the von Neumann entropy, the entropy-proxy captures essential features of information mixing and irreversibility. Expressions of the typical form $S(x,t) = p \ln(p + \varepsilon)$

originate from Shannon's foundational work on the information theory [76] and have long been used as local entropy densities in the lattice models and cellular automata [92].

The observed monotonic growth of the entropy-proxy in macrocircuit regimes supports the interpretation that the arrow of time emerges from information loss, not from fundamental time-asymmetric laws. This is consistent with:

- (1) Coarse-graining arguments in statistical mechanics [2,64,96], (2) Data-processing inequalities in quantum information theory [50], (3) Decoherence-based approaches to classical emergence [15].

Crucially, entropy growth in the present model does not require stochasticity or randomness. It arises from those deterministic nonlinear dynamics combined with selective observables, reinforcing the view that classical thermodynamics is compatible with underlying reversible laws.

Lorentz Violation, Discreteness, and Sub-Continuum Structure

The inclusion of higher-order spatial derivatives introduces controlled Lorentz-violating corrections at the small scales. While such terms are negligible at the macroscopic resolutions, they become significant near the lattice cutoff. This behaviour is consistent with also the wide class of emergent relativity scenarios, within which Lorentz symmetry would be only approximate rather than fundamental [37,44,49].

From this perspective, Lorentz invariance appears as a large-scale emergent symmetry, that would be restored only after coarse graining over microscopic discreteness. Similar ideas have already been explored in analogue gravity systems, lattice field theories, and quantum gravity phenomenology [7,21,85]. Present results suggest that modest Lorentz violations at the sub- $(\ell_c \sim 10^{-16} m)$ scales need not contradict relativistic physics, provided they remain confined to unobservable microcircuits.

Relation to Pre-Geometric and Discrete Spacetime Approaches

Overall, typical separation between microcircuits and macrocircuits resonates strongly with the pre-geometric approaches to spacetime, where spacetime itself is not fundamental but emerges from typically well within the deeper combinatorial or informational structures. In causal set theory, spacetime points arise from partially ordered sets [14]; in causal dynamical triangulations, classical geometry emerges only after coarse graining over simplicial microstructures [2].

Within this very context, the present model can be interpreted as a pre-geometric fields' architecture, where:

- Microcircuits encode reversible quantum information flow,
- Macrocircuits encode events, causality, and temporal ordering,

- Spacetime observables emerge from thresholded, coarse-grained dynamics.

The emergence of persistent particle clusters and entropy gradients may thus be viewed as early indicators of emergent locality and causal structure, rather than as the fundamental properties within underlying lattice.

Limitations and Sensitivities

Several limitations must be emphasized, despite the robustness of the qualitative results:

- The simulations employ classical scalar fields with entropy-like diagnostics. Genuine quantum entanglement and operator-valued observables are not explicitly representable.
- Phenomenological Thresholding

Particle-creation threshold (ρ_c) is introduced phenomenologically. While physically motivated, such a derivation from microscopic quantum principles will be open problem.

- The Finite-Size and Discretization Effects

Lattice anisotropy, boundary conditions, and higher-order finite differences may introduce artifacts that are absent in continuum quantum field theory.

- With having the Restricted Field Content

Absence of gauge fields, fermions, and spin degrees of freedom limits direct comparisons with realistic particle physics.

These constraints, however, do not undermine the conceptual conclusions but they define a clear roadmap for advancing further to future refinement.

Outlook and Future Directions

Several promising appropriate directions naturally follow from the present work:

- **Fully Quantum Implementations:** Appropriately incorporating tensor-network methods, matrix-product states, or explicitly unitary QCA operators would allow direct access to the entanglement dynamics also having typically the von Neumann entropy [13,61].
- **Gauge Fields and Spinor Automata:** Extending framework to include U (1), SU (2), or Dirac-like QCA constructions would be yielding the emergent fermionic excitations and richer particle phenomenology [5,13].
- **Renormalization and Multi-Scale Analysis:** A systematic renormalization-group treatment could clarify how reversible microcircuits flow toward irreversible macrocircuits, connecting the present results to universality and scaling theory [17,94].
- **Quantum Gravity and Emergent Time:** Via coupling the model to causal sets, spin foams, or dynamical

triangulations may illuminate the origin of time asymmetry in quantum gravity contexts [2,14,60].

- **Having Computational with Information-Theoretic Applications:** The framework may also serve as a testbed for reversible computation, quantum simulation, as well as the information-theoretic models of matter [10,52].

General Concluding Perspective

In summary, this work provides a constructive and computationally explicit demonstration that macroscopic irreversibility, particle stability, and entropy production can emerge from potentially possible fundamentally reversible quantum lattice dynamics. The key mechanism will not evolve out of typical dissipation or randomness, but scale-dependent information accessibility that would be encoded through the nonlinear interactions and QCA-style event rules.

These results support a broader paradigm in which particles, spacetime events, and arrow of time are emergent phenomena, rooted in deeper discrete informational substrates. Research efforts with continued progressive development along this direction may help bridge quantum information theory, lattice field models, condensed matter analogues, and quantum gravity into a well unified proper framework for emergent classical reality.

Summary Conclusions with Project Research Proceeding

This work establishes that discrete, reversible, and information-theoretically grounded lattice architectures naturally generate emergent particles and macroscopic irreversibility. The results provide a thorough concrete computational demonstration that the arrow of time, classical complexity, and localized matter need not be fundamental, but may instead originate from deeper reversible microdynamics operating on discrete spacetime structures. By bridging variational lattice physics, quantum cellular automata, and entropy-based diagnostics, the framework developed here offers both a conceptual foundation and a practical numerical laboratory for exploring further emergent classicality, pre-geometric physics, as well as the informational origins of that spacetime and matter. Continued development along these lines may contribute to unifying ideas out from quantum information theory, condensed-matter physics, and quantum gravity into a coherent picture of emergent physical law.

Summary of Principal Results

Within this work, we have introduced and analyzed the hybrid discrete framework that unifies typically variational lattice field theory with quantum cellular automaton

(QCA)-inspired event encoding investigating emergence of particles, entropy production, and macroscopic observable irreversibility from out of fundamentally reversible dynamics. Here, the model combines also typical nonlinear scalar-field evolution on discrete spacetime lattices with the local, causal threshold rules that translate continuous overall general field dynamics into discrete particle-like events.

Principal findings may be summarized as follows:

- **Microscopic Reversibility out from Variational Dynamics:** At spatial and temporal resolutions below a critical scale ($\ell_c \sim 10^{-16} m$), the lattice inner dynamics exhibit stable, reversible behaviour characterized by coherent waves as well as soliton-like excitations. Energy and entropy-proxy measures remain overall approximately conserved, that provide consistency with discrete variational mechanics and unitary QCA principles. This regime constitutes a reversible quantum lattice microcircuit, demonstrating that discrete spacetime dynamics can faithfully reproduce reversible microscopic evolution.
- **Emergent Particle Events via Local Thresholding:** Particle-like excitations are not introduced as fundamental degrees of freedom but that will instead emerge dynamically through local energy-density thresholds applied to the evolving fields. These events exhibit persistence, clustering, and scale dependence, supporting the interpretation that particles can arise as emergent structures from nonlinear general fields that involve interactions rather than as primitive entities.
- **Entropy Growth and Macroscopic Irreversibility:** An entropy-proxy functional based on local field intensity reveals a sharp transition from oscillatory, reversible overall behavior at small scales to monotonic entropy growth at larger scales. This marks the onset of an effective macrocircuit regime, characterized by excitation coalescence, particle clustering, and irreversible dynamics. Notably, this arrow of time arises without external noise, dissipation, or imposed coarse graining.
- **The Dual-Scale Dynamical Structure:** Having the same underlying deterministic and reversible lattice equations support both reversible microcircuits and irreversible macrocircuits. Separation between these regimes is controlled then by scale and information accessibility rather than by changes to the typical fundamental laws. Thus, this will provide a concrete realization of a dual time-scale lattice theory, in which microscopic reversibility and macroscopic irreversibility coexist naturally.

Taken together, these results demonstrate that macroscopic irreversibility, particle stability, as well as

entropy production can emerge dynamically from reversible microscopic dynamics, thereby reinforcing view that classical behavior and the arrow of time need not be fundamental ingredients of physical law.

Implications for Emergent Physics

Overall, all the framework developed here has several broader implications. First, it supports higher information-theoretic and quantum-foundational perspectives in which irreversibility is potentially understood possibly because of restricted observability as well as nonlinear information processing, rather than explicit dissipation. Second, it provides a constructive mechanism for emergent matter within discrete field architectures, closely aligned to the approaches within quantum cellular automata, condensed-matter analogues, as well as what may presently constitute possible deterministic interpretations of quantum mechanics.

Moreover, the appearance of Lorentz-violating corrections confined to sub- ($\ell_c \sim 10^{-16} m$) scales suggests

that relativistic symmetry may be an emergent, large-scale property rather than a truly fundamental general feature of microscopic dynamics. Thus, within this sense, the model offers a testbed for pre-geometric physics, where spacetime structure, particles, as well as temporal directionality arise from deeper discrete informational substrates.

Outlook and the Future Research Directions

The present study opens several promising avenues for future investigations:

- **The Fully Quantum Extensions:** Replacing classical scalar fields with explicitly unitary QCA rules, tensor-network evolutions, or matrix-product-state architectures would enable direct simulation of the quantum entanglement, observable interference, and von Neumann entropy. This step is essential for establishing a genuinely-quantum discrete field theory.
- **Gauge Fields, the Fermions, and Topology:** Extensions to multi-component fields, spinor degrees of freedom, and gauge interactions could test whether the observed micro-macro duality persists in more realistic settings. Such generalizations may also allow for the emergence of topological charges, typically observable fermionic excitations, and richer particle phenomenology.
- **Renormalization and Multi-Scale Analysis:** Subsequently, developing systematic real-space or information-theoretic renormalizations procedures within this very framework would clarify how reversible microcircuits coarse-grain into possible irreversible macrocircuits. This could establish discrete analogue for

- eventual thermodynamic emergence and universality.
- Overall Connections to Quantum Gravity and Discrete Spacetime:** Embedding the present dynamics within causal-set theory, dynamical triangulations, or graph-based QCA architectures may shed light on the origin of spacetime locality, causal structure, and gravitational time asymmetry from pre-geometric dynamics.
- Machine-Learning-Assisted Discovery:** Machine-learning techniques, including neural-network quantum states and developing potential unsupervised phase-detection algorithms, could be employed to identify current hidden dynamical phases, optimize particle-detection criteria, and explore large parameter spaces efficiently.

Acknowledgments

The author acknowledges the foundational contributions of Engineering Inc. and International Operational Teknet Earth Global for establishing an integrated platform that has enabled the successful development and dissemination of several international scientific projects. The ongoing constructive engagement of researchers across global forums, particularly through ResearchGate, virtual symposia, and conferences such as the 2025 Budapest TEGS Global Physics Conference, has provided essential channels for the exchange of ideas and scholarly advancement, further shared on YouTube TEKNET EARTH GLOBAL SYMPOSIA (TEGS) website:

<https://www.youtube.com/channel/UCdUnenH0oEFiSxivgVqLYw>

Especially, the author further recognizes the scientific insight with ongoing collaborative support of distinguished peer colleagues, including especially Dr. Emmanouil Markoulakis of the Hellenic Mediterranean University, Greece for coauthored investigations within research quantum astrophysics, and Dr. Christopher O'Neill of the Cataphysics Group, Ireland for his technical contributions and organizational coauthoring participation in perpetual sessions with joint conference initiatives. The author's appreciation is also extended to Drs. Manuel Malaver, John Hodge, Emory Taylor, Wenzhong Zhang, Laszlo Horvath, and Dr. Muhammet Kurulay with organizational leadership enhancing global scientific engagement forums, enriching the broader research efforts, while supporting achievable goals. Gratitude is conveyed to progressive peer-reviewed journals that have facilitated the publication of the related studies through rigorous evaluator processes. The use of open-source Artificial Intelligence (AI)-enabled tools as well as scientific software advanced computational resources has also likewise supported precise visualization and analysis underpinning this work to achieve simulations graphics.

References

1. Alicki R, Lendi K (2007) Quantum Dynamical Semigroups and Applications 2nd (Edn.), Springer, Berlin.
2. Ambjørn J, Jurkiewicz J, Loll R (2005) Reconstructing the universe. *Physical Review D* 72: 064014.
3. Arrighi P (2019) An overview of quantum cellular automata. *Natural Computing* 18: 885-899.
4. Arrighi P, Nesme V, Werner R (2011) Unitarity plus causality implies localizability. *Journal of Computer and System Sciences* 77: 372-378.
5. Arrighi P, Nesme V, Werner R (2011) Unitary evolution and causal structures in discrete space-time. *Physical Review A* 83: 052338.
6. Bak P, Tang C, Wiesenfeld K (1988) Self-organized criticality. *Physical Review A* 38: 364-374.
7. Barceló C, Liberati S, Visser M (2011) Analogue gravity. *Living Reviews in Relativity* 14(3).
8. Barbour J, Koslowski T, Mercati F (2014) Identification of a gravitational arrow of time. *Physical Review Letters* 113: 181101.
9. Bekenstein JD (1973) Black holes and entropy. *Physical Review D* 7: 2333-2346.
10. Bennett CH (1973) Logical reversibility of computation. *IBM Journal of Research and Development* 17: 525-532.
11. Berezinskii VL (1971) Destruction of long-range order in one-dimensional and two-dimensional systems having a continuous symmetry group I. *Soviet Physics JETP* 32: 493-500.
12. Bertschinger E (1998) Simulations of structure formation in the universe. *Annual Review of Astronomy and Astrophysics* 36: 599-654.
13. Bisio A, D'Ariano GM, Tosini A (2015) Quantum field as a quantum cellular automaton: The Dirac free evolution in one dimension. *Annals of Physics* 354: 244-264.
14. Bombelli L, Lee J, Meyer D, Sorkin RD (1987) Space-time as a causal set. *Physical Review Letters* 59: 521-524.
15. Breuer HP, Petruccione F (2002) The Theory of Open Quantum Systems. Oxford University Press, United Kingdom.
16. Buchert T (2000) On average properties of inhomogeneous fluids in general relativity. *General Relativity and Gravitation* 32: 105-125.

17. Cardy J (1996) Scaling and Renormalization in Statistical Physics. Cambridge University Press, United Kingdom.
18. Carroll SM (2010) From Eternity to Here: The Quest for the Ultimate Theory of Time. New York.
19. Chaikin PM, Lubensky TC (1995) Principles of Condensed Matter Physics. Cambridge University Press, United Kingdom.
20. Choi S, Bao Y, Qi XL, Altman E (2020) Quantum error correction in scrambling dynamics and measurement-induced phase transition. *Physical Review Letters* 125: 030505.
21. Collins J, Perez A, Sudarsky D, Urrutia LF, Vucetich H (2004) Lorentz invariance and quantum gravity: An additional fine-tuning problem? *Physical Review Letters* 93: 191301.
22. Cover TM, Thomas JA (2006) Elements of Information Theory 2nd (Edn.), Wiley-Interscience, New York.
23. Creutz M (1983) Quarks, Gluons and Lattices. Cambridge University Press, United Kingdom.
24. Dauxois T, Peyrard M (2006) Physics of Solitons. Cambridge University Press, United Kingdom.
25. Dennis MR, O'Holleran K, Padgett MJ (2009) Singular optics: Optical vortices and polarization singularities. *Progress in Optics* 53: 293-363.
26. Faddeev LD, Takhtajan LA (2007) Hamiltonian Methods in the Theory of Solitons. Springer, Berlin.
27. Ginzburg VL, Landau LD (1950) On the theory of superconductivity. *ZhETF* 20: 1064-1082.
28. Goldenfeld N (1992) Lectures on Phase Transitions and the Renormalization Group. Addison-Wesley, USA.
29. Gorini V, Kossakowski A, Sudarshan ECG (1976) Completely positive dynamical semigroups of N-level systems. *Journal of Mathematical Physics* 17: 821-825.
30. Haake F (2010) Quantum Signatures of Chaos. Springer 3.
31. Hastings MB, Wen XG (2005) Quasi-adiabatic continuation of quantum states. *Physical Review B* 72: 045141.
32. Hawking SW (1975) Particle creation by black holes. *Communications in Mathematical Physics* 43: 199-220.
33. Hindmarsh M, Kibble TWB (1995) Cosmic strings. *Reports on Progress in Physics* 58: 477-562.
34. Hooft Gt (2016) The Cellular Automaton Interpretation of Quantum Mechanics. Springer 185: 1-296.
35. Iyer R (2025) Early Universe Magneto-Gravitational Coupling Genesis Physics: Part I. *Open Journal of Astronomy* 3(2): 000165.
36. Jacobson T (1995) Thermodynamics of spacetime. *Physical Review Letters* 75: 1260-1263.
37. Jacobson T, Liberati S, Mattingly D (2006) Lorentz violation at high energy. *Annals of Physics* 321: 150-196.
38. Joos E, Zeh HD, Kiefer C, Giulini D, Kupsch J, et al., (2003) Decoherence and the Appearance of a Classical World in Quantum Theory. Springer.
39. Jordan SP, Le KSM, Preskill J (2012) Quantum algorithms for quantum field theories. *Science* 336: 1130-1133.
40. Kadanoff LP (1966) Scaling laws for Ising models near Tc. *Physics Physique Fizika* 2: 263-272.
41. Kadanoff LP (2000) Statistical Physics. World Scientific.
42. Kibble TWB (1976) Topology of cosmic domains and strings. *Journal of Physics A* 9: 1387-1398.
43. Kolb EW, Turner MS (1990) The Early Universe. Addison-Wesley, USA.
44. Kostelecký VA, Samuel S (1989) Spontaneous breaking of Lorentz symmetry. *Physical Review D* 39: 683-685.
45. Kosterlitz JM, Thouless DJ (1973) Ordering, metastability and phase transitions in two-dimensional systems. *Journal of Physics C: Solid State Physics* 6: 1181-1203.
46. Kraus K (1971) General state changes in quantum theory. *Annals of Physics* 64: 311-335.
47. Landauer R (1991) Information is physical. *Physics Today* 44(5): 23-29.
48. Li Y, Chen X, Fisher MPA (2018) Quantum Zeno effect and the many-body entanglement transition. *Physical Review B* 98: 205136.
49. Liberati S (2013) Tests of Lorentz invariance. *Classical and Quantum Gravity* 30: 133001.
50. Lindblad G (1975) Completely positive maps and entropy inequalities. *Communications in Mathematical Physics* 40: 147-151.
51. Lindblad G (1976) On the generators of quantum dynamical semigroups. *Communications in Mathematical Physics* 48: 119-130.

52. Lloyd S (2006) Programming the Universe. Knopf.

53. Lüders G (1951) About the change of state due to the measurement process. *Annalen der Physik* 443: 322-328.

54. Marsden JE, West M (2001) Discrete mechanics and variational integrators. *Acta Numerica* 10: 357-514.

55. Manton N, Sutcliffe P (2004) Topological Solitons. Cambridge University Press, United Kingdom.

56. Mermin ND (1979) The topological theory of defects. *Reviews of Modern Physics* 51: 591-648.

57. Nelson DR (2002) Defects and Geometry in Condensed Matter Physics. Cambridge University Press, United Kingdom.

58. Nielsen MA, Chuang IL (2000) Quantum Computation and Quantum Information. Cambridge University Press, United Kingdom.

59. Noether E (1918) Invariant variation problems. *Nachrichten von der Gesellschaft der Wissenschaften zu Göttingen* 235-257.

60. Oriti D (2014) Disappearance and emergence of spacetime. *Studies in History and Philosophy of Modern Physics* 46: 186-199.

61. Orús R (2014) Tensor networks. *Annals of Physics* 349: 117-158.

62. Page DN, Wootters WK (1983) Evolution without evolution. *Physical Review D* 27: 2885-2892.

63. Padmanabhan T (2010) Thermodynamical aspects of gravity. *Reports on Progress in Physics* 73: 046901.

64. Penrose O (1979) Foundations of Statistical Mechanics. Pergamon.

65. Penrose R (1989) Difficulties with inflationary cosmology. *Annals of the NYAS* 571: 249-264.

66. Peres A (1995) Quantum Theory: Concepts and Methods. Kluwer.

67. Peskin ME, Schroeder DV (1995) An Introduction to Quantum Field Theory. Addison-Wesley.

68. Petz D (2008) Quantum Information Theory and Quantum Statistics. Springer.

69. Preskill J (2018) Quantum computing in the NISQ era. *Quantum* 2: 79.

70. Prosen T (2002) General quantum chaos. *Physical Review E* 65: 036208.

71. Rajaraman R (1982) Solitons and Instantons. North-Holland.

72. Recami E (1986) Classical tachyons. *Rivista del Nuovo Cimento* 9(6): 1-178.

73. Rothe HJ (2012) Lattice Gauge Theories. World Scientific 4.

74. Sakurai JJ, Napolitano J (2017) Modern Quantum Mechanics. Cambridge University Press, United Kingdom, 2.

75. Schlosshauer M (2007) Decoherence and the Quantum-to-Classical Transition. Springer pp: 13-114.

76. Shannon CE (1948) A mathematical theory of communication. *Bell System Technical Journal* 27(3): 379-423.

77. Skinner B, Ruhman J, Nahum A (2019) Measurement-induced phase transitions. *Physical Review X* 9: 031009.

78. Sorkin RD (2005) Causal sets: Discrete gravity. In *Lectures on Quantum Gravity*. Springer pp: 305-327.

79. Springel V (2005) The cosmological simulation code GADGET-2. *MNRAS* 364: 1105-1134.

80. Srednicki M (2007) Quantum Field Theory. Cambridge University Press, United Kingdom.

81. Stanley HE (1971) Introduction to Phase Transitions and Critical Phenomena. Oxford University Press, USA.

82. Succi S (2018) The Lattice Boltzmann Equation. Oxford University Press, USA.

83. Uhlmann A (1977) Relative entropy. *Communications in Mathematical Physics* 54: 21-32.

84. Verlinde E (2011) On the origin of gravity. *Journal of High Energy Physics* 4: 29.

85. Volovik GE (2003) The Universe in a Helium Droplet. Oxford University Press, USA.

86. von Neumann J (1955) Mathematical Foundations of Quantum Mechanics. Princeton University Press, Springer, Berlin.

87. Wald RM (1994) Quantum Field Theory in Curved Spacetime. University of Chicago Press, USA.

88. Wehrl A (1978) General properties of entropy. *Reviews*

of Modern Physics 50: 221-260.

89. Weinberg S (1995) The Quantum Theory of Fields. Cambridge University Press, USA Vol 1.

90. Wilson KG, Kogut J (1974) The renormalization group and the ϵ expansion. Physics Reports 12(1): 75-199.

91. Wolfram S (1983) Statistical mechanics of cellular automata. Reviews of Modern Physics 55: 601-644.

92. Wolfram S (1984) Universality and complexity in cellular automata. Physica D 10(1-2): 1-35.

93. Zamolodchikov AB (1986) Irreversibility of the RG flow. JETP Letters 43: 730-732.

94. Zeh HD (2007) The Physical Basis of the Direction of Time 5th (Edn.), Springer.

95. Zinn-Justin J (2002) Quantum Field Theory and Critical Phenomena. Oxford University Press, USA, 4.

96. Zurek WH (2003) Decoherence, einselection and the quantum origins of the classical. Reviews of Modern Physics 75: 715-775.